A Statistical Study of the Maximum Ground Motion in Strong Earthquakes

By

Hisao GOTO* and Hiroyuki KAMEDA**

(Received June 28, 1967)

This paper presents the results of a theoretical analysis of the statistical properties of the maximum ground motions in strong earthquakes. The statistical model of earthquakes is proposed so as to be consistent with the past records of occurrence of earthquakes and with strong motion accelerograms, on the basis of which the methods are discussed to find the probability distribution of the maximum ground motion in a single earthquake and that for a certain future period. Numerical results are given in the form of charts and seismic maps.

1. Introduction

From the randomness of the sequence of strong earthquakes and of the ground motion in earthquakes, it is considered essential to make a statistical evaluation of the intensity of the earthquake for which structures are to be designed. The structure may be designed for the earthquake with the maximum ground acceleration corresponding to a certain assigned probability of excess or for a set of earthquakes with a certain assigned r.m.s. intensity. Whatever the measure of the earthquake intensity may be, there must be provided sufficient statistical information based on the data of occurrence of past strong earthquakes and seismograph records. Due to the fact, however, that in most districts of Japan destructive earthquakes occur at intervals of several tens or a hundred and several tens of years, the record of earthquakes before modern science is required. However, one can readily understand that it is extremely difficult to obtain a complete one of such a record. On the other hand, the observation projects of strong earthquake motions started only in the 1930's in the U.S.A. and in the 1950's in Japan; so that it can not be expected that we shall be provided with all typical seismograph records of strong earthquakes in the near future. What we can do, therefore, is to make the best use of the data available at present. But the studies in this field so far

* Department of Transportation Engineering
** Department of Civil Engineering

published after the classical paper by H. Kawasumi[1] seem to be rare. Kawasumi clarified the past seismic activities throughout Japan from the record of occurrence of earthquakes collected from old documents, and prepared the seismic map showing the maximum earthquake acceleration expected to occur in 75, 100 and 200 years computed by the method of the return period. In his paper, the list of the dates, locations and magnitudes of past strong earthquakes is especially complemented, and a great part of the data of past earthquakes used in this study is essentially based on it.

On the other hand, it would pose a problem to apply the idea of the return period to this list. For, it would not indicate all strong earthquakes which occurred in the period studied. Fig. 1, for example, shows the number of earthquakes felt to be of intensity V or stronger in the JMA scale* in every 200 years in Tokyo and Kyoto computed by Kawasumi's method[1] on the basis of the list of destructive earthquakes in the Chronological Table of Science, 1966** (edited by the Tokyo Astronomical Observatory). It is noted that for the most recent 200 years far more earthquakes are recorded than for other ages. It would be more reasonable to interpret this as being that some strong earthquakes which occurred in older ages are missing in this record than to believe that it is a precise description of past seismic activities. The idea that the accuracy of this record is affected by political or social conditions would be supported, for example, by the fact that the number of earthquakes in Tokyo increases suddenly in the Edo Era, while fairly many earthquakes are recorded for Kyoto even in earlier times which has long been the political and cultural centre of Japan. Thus it could be concluded that inference of the future earthquake danger should be based primarily on the record of recent seismic activities, and in this view of the problem, it is likely that direct application of the method of the return period may underestimate the future seismic activity.

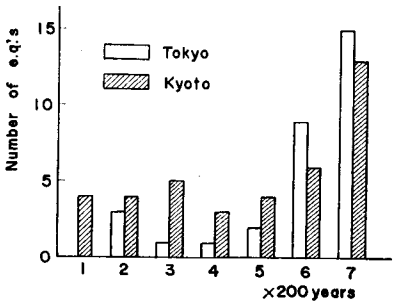

Fig. 1. Number of Earthquakes in Every 200 years ($I \geqq V$; A.D. 565 ~1964).

I. Muramatsu pointed out this problem and computed the maximum ground velocity expected in 50 years by the method of the return period applied to the

* Unless otherwise is stated, the phrases "intensity V, intensity VI, etc." shall be used to represent the earthquake intensity in the JMA (Japan Meteorological Agency) scale.

** Most part of its record of earthquakes before 1950 coincides with Kawasumi's list.

earthquakes which had occurred after 1868.[2] However, the number of earthquakes used in his paper has naturally decreased to less than half of that in Kawasumi's paper. Thus Muramatsu's paper could not be said to have made the best use of those precious records of past earthquakes.

Besides, the method of return period enables one to estimate only the expected value of the maximum ground motion, and can not aid him to derive its probability distribution which is a more essential statistical information for designers, since the probability distribution for a unit period is not known.

The present study has been carried out in search of a more reasonable method which could solve these problems. First, the occurrence of earthquakes is treated as the successive Bernoulli trials. The ground motion, on the other hand, is analyzed in the language of the theory of random processes from which the probability distribution of the maximum ground motion in a single earthquake is derived. From the results of these analyses, the probability distribution and the expected value of the maximum ground motion at a certain locality in a certain future period are obtained.

2. Statistical Model of Earthquakes

(1) Sequence of Earthquakes

Divide the past ages into r intervals $B_1, B_2, \cdots, B_r$ of arbitrary length $S_1, S_2, \cdots, S_r$, respectively, and suppose that at a certain locality N_k, $(k=1, 2, \cdots, r)$,

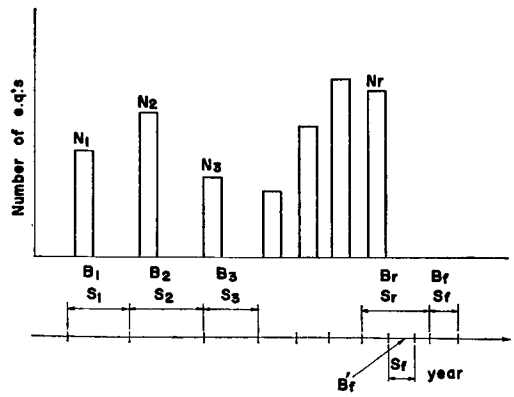

Fig. 2. Division of Time Axis and Number of Earthquakes.

earthquakes occurred in the interval B_k, as shown in Fig. 2. The total number N of past earthquakes for this locality is then given by

$$N = \sum_{k=1}^{r} N_k$$

If $n_{I1}, n_{I2}, \cdots, n_{Im}$ of these N earthquakes were felt to be of intensity $I_1, I_2, \cdots, I_m$, respectively, N is represented in terms of n_{Il}, $(l=1, 2, \cdots, m)$, by

$$N = \sum_{l=1}^{m} n_{Il}$$

Our statistical model for this record shall be described as follows: it is assumed that this record is a realization of N Bernoulli trials of which $n_{I1}, n_{I2}, \cdots, n_{Im}$ trials are made for earthquakes of intensity $I_1, I_2, \cdots, I_m$, respectively. This statement implies that the intensity of earthquakes in all trials are statistically independent. As a matter of fact, there would be some correlation between the intensities of successive strong earthquakes. The data of past earthquakes, however, are not sufficient to allow us to detect this correlation. Hence the foregoing assumption would be what we can do best at present. In addition, it would be natural to assume that the maximum ground motions in all earthquakes are also statistically independent, and this assumption shall be used in the next chapter.

The probability P_k that the earthquake in one Bernoulli trial will occur in the interval B_k is approximately given by

$$P_k = \frac{N_k}{N} \qquad \cdots\cdots\cdots\cdots(1)$$

This P_k is considered to represent the moment of the interval B_k in the whole record. By making a weighted evaluation of earthquake danger in each interval with the aid of such P_k, the usefulness of the record of past earthquakes whose accuracy is likely to vary with ages would be improved to a considerable extent.

If we assume that the intensity of seismic activity in the most recent interval B_r will not vary through a future interval B_f of length S_f for which the earthquake danger is to be estimated, then it suffices to analyze a subinterval B_f' of B_r of length S_f. The probability P_f that the earthquake will occur in the interval B_f' in one Bernoulli trial is given from Eq. (1) by

$$P_f = \frac{S_f}{S_r} P_r = \frac{N_r S_f}{N S_r} \qquad \cdots\cdots\cdots\cdots(2)$$

From the above discussions the probability $P_c(k_{I1}, k_{I2}, \cdots, k_{Im})$ that $k_{I1}, k_{I2}, \cdots, k_{Im}$ earthquakes of intensity $I_1, I_2, \cdots, I_m$, respectively, will occur in the interval B_f', hence in B_f also, is given by

$$P_c(k_{I1}, k_{I2}, \cdots, k_{Im}) = \mathrm{P}\Big[\bigcap_{j=1}^{m} (k_{Ij}\text{e.q.'s of intensity } I_j \subset B_f')\Big]$$

$$= \prod_{j=1}^{m} \left\{ \binom{n_{Ij}}{k_{Ij}} P_f^{k_{Ij}} (1-P_f)^{n_{Ij}-k_{Ij}} \right\} = \prod_{j=1}^{m} \mathrm{b}(k_{Ij}; n_{Ij}, P_f) \qquad \cdots\cdots\cdots\cdots(3)$$

Here P[R] denotes the probability of an event R, and

$$\mathrm{b}(k;\, n,\, p) = \binom{n}{k} p^k (1-p)^{n-k}$$

is the binomial distribution function. Summing up Eq. (3) for all k_I, we have

$$\begin{aligned} &\mathrm{P}[(\text{no e.q.} \subset B_f') \bigcup (\text{at least one e.q.} \subset B_f')] \\ &= \sum_{k_{I1}=0}^{n_{I1}} \sum_{k_{I2}=0}^{n_{I2}} \cdots \sum_{k_{Im}=0}^{n_{Im}} P_c(k_{I1},\, k_{I2},\cdots,\, k_{Im}) \\ &= \sum_{k_{I1}=0}^{n_{I1}} \sum_{k_{I2}=0}^{n_{I2}} \cdots \sum_{k_{Im}=0}^{n_{Im}} \prod_{j=1}^{m} \mathrm{b}(k_{Ij};\, n_{Ij},\, P_f) = 1 \end{aligned}$$

thus proving that Eq. (3) satisfies the condition of total probability.

(2) Description of the Ground Motion

As the strong motion accelerograph records were obtained, the characteristics of the strong earthquake motion have gradually been disclosed. So far, it has been taken appropriate to assume that 1) the wave form of the ground acceleration in strong earthquakes is highly irregular, that 2) distribution of amplitude of some strong earthquake motions is nearly Gaussian[3),4)] and that 3) although the time history of a strong earthquake motion is statistically nonstationary, its strongest part of duration of, say several or ten and several seconds, are fairly stationary as we see in Fig. 3. Since we are concerned with the maximum ground motion, it would be reasonable to deal only with this strong part of the seismogram.

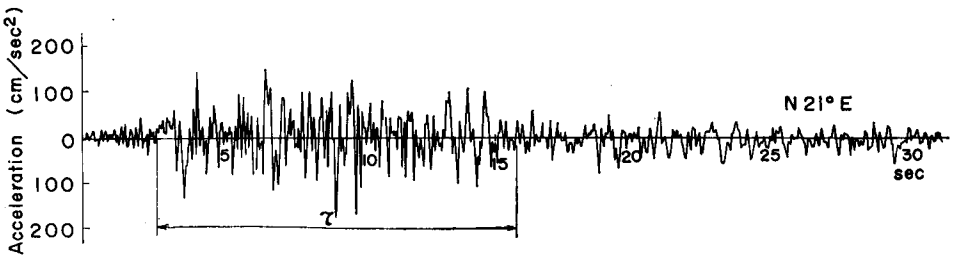

Fig. 3. Accelerogram for the Taft, Calif., U.S.A. Earthquake of July 21, 1952, Component N21°E.

In the present study, the earthquake acceleration $x(t)$ shall be represented by

$$x(t) = \beta f(t;\, \tau)\, g(t) \qquad \cdots\cdots\cdots\cdots (4)$$

where $g(t)$ is a stationary random process with zero mean value and the variance of unity, and β is a constant value with the dimension of acceleration. The function $f(t;\, \tau)$ is represented by

$$f(t;\tau)=u_-(t)-u_+(t-\tau)=\begin{cases}1; 0\leqq t\leqq\tau\\ 0; t<0,\quad t>\tau\end{cases} \qquad \cdots\cdots(5)$$

in which $u_\pm(t)$ are the asymmetrical unit step functions. Thus $x(t)$ is a stationary random process with zero mean and the variance β^2 in the interval $0\leqq t\leqq\tau$. The time derivative $\dot{f}(t;\tau)$ of $f(t;\tau)$ obviously takes the form

$$\dot{f}(t;\tau)=\delta_-(t)-\delta_+(t-\tau) \qquad \cdots\cdots(6)$$

where $\delta_\pm(t)$ are the asymmetrical impulse functions.

If we further assume the Gaussian distribution for $g(t)$, hence also for $x(t)$, then the probability density $\phi(x;t)$ of $x(t)$ and the joint probability density $\phi_j(x,\dot{x};t)$ of $x(t)$ and $\dot{x}(t)$ are given by

$$\phi(x;t)=\frac{1}{\sqrt{2\pi}\sigma_1}\exp\left\{-\frac{1}{2}\left(\frac{x}{\sigma_1}\right)^2\right\} \qquad \cdots\cdots(7)$$

$$\phi_j(x,\dot{x};t)=\frac{1}{2\pi\sigma_1\sigma_2\sqrt{1-\rho_{12}^2}}\exp\left[-\frac{1}{2(1-\rho_{12}^2)}\left\{\left(\frac{x}{\sigma_1}\right)^2-2\rho_{12}\left(\frac{x}{\sigma_1}\right)\left(\frac{\dot{x}}{\sigma_2}\right)+\left(\frac{\dot{x}}{\sigma_2}\right)^2\right\}\right] \qquad \cdots\cdots(8)$$

where σ_1 and σ_2 are the standard deviations of $x(t)$ and $\dot{x}(t)$, respectively, and ρ_{12} is the correlation coefficient between $x(t)$ and $\dot{x}(t)$, which are represented as follows:

$$\left.\begin{aligned}\sigma_1=\sigma_1(t)&=\left\{\mathrm{E}[x^2(t)]\right\}^{1/2}=\beta\sigma_{g_1}f(t;\tau)\\ \sigma_2=\sigma_2(t)&=\left\{[\mathrm{E}\dot{x}^2(t)]\right\}^{1/2}=\beta\left\{\sigma_{g_1}^2\dot{f}^2(t;\tau)+\sigma_{g_2}^2f^2(t;\tau)\right\}^{1/2}\\ \rho_{12}=\rho_{12}(t)&=\frac{\mathrm{E}[x(t)\,\dot{x}(t)]}{\sigma_1\sigma_2}=\beta^2\frac{\sigma_{g_1}^2}{\sigma_1\sigma_2}f(t;\tau)\dot{f}(t;\tau)\end{aligned}\right\} \qquad \cdots\cdots(9)$$

Here $\mathrm{E}[z]$ denotes the mathematical expectation of a random variable z. The quantities σ_{g_1} and σ_{g_2} are the standard deviations of $g(t)$ and $\dot{g}(t)$, respectively, and are computed from

$$\sigma_{g_1}^2=\mathrm{E}[g^2(t)]=\int_0^\infty S_g(\omega)\,d\omega \qquad \cdots\cdots(10)$$

and

$$\sigma_{g_2}^2=\mathrm{E}[\dot{g}^2(t)]=\int_0^\infty \omega^2 S_g(\omega)\,d\omega \qquad \cdots\cdots(11)$$

where $S_g(\omega)$ is the power spectrum of $g(t)$. The resonance curve of a single-degree-of-freedom oscillator is frequently used to represent the power spectrum of the

earthquake acceleration. With this assumption, however, the infinite integral in Eq. (11) diverges. Hence there needs be proposed a new formula for $S_g(\omega)$.

Fig. 4 shows the semi-logarithmic plots of the power spectrum of the ground displacements obtained by integration of accelerograms recorded in the U.S.A. with the maximum accelerations of some 200~300 cm/sec^2, which had been so normalized in advance of integration as to have the zero mean and the variance of unity. It

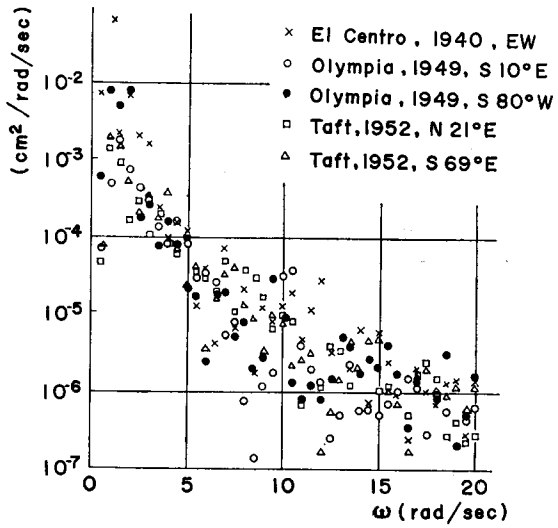

Fig. 4. Power Spectrum of Ground Displacement in Earthquakes.

is noted from this figure that the power spectrum of the ground displacement dies out linearly on the whole with increasing frequency. Hence in the linear scale, it has exponential characteristics. On the basis of these arguments, $S_g(\omega)$ whose shape is similar to that of the power spectrum of the ground acceleration shall be represented in the following form:

$$S_g(\omega) = \frac{128}{3\omega_0}\left(\frac{\omega}{\omega_0}\right)^4 e^{-4\frac{\omega}{\omega_0}} \qquad \cdots\cdots\cdots\cdots(12)$$

where ω_0 is the predominant frequency. This $S_g(\omega)$ has a single peak at $\omega=\omega_0$ as shown in Fig. 5. The auto-correlation function $R(\tau)$ associated with Eq. (12) is obtained as its Fourier inverse transform:

$$R(\tau) = \frac{1}{{\sigma_{g_1}}^2}\int_0^\infty S_g(\omega)\cos\omega\tau\, d\omega = \left\{1-10\left(\frac{\omega_0\tau}{4}\right)^2+5\left(\frac{\omega_0\tau}{4}\right)^4\right\}\Big/\left\{1+\left(\frac{\omega_0\tau}{4}\right)^2\right\}^5 \qquad \cdots\cdots\cdots\cdots(13)$$

Substitution of Eq. (12) into Eqs. (10) and (11) yields

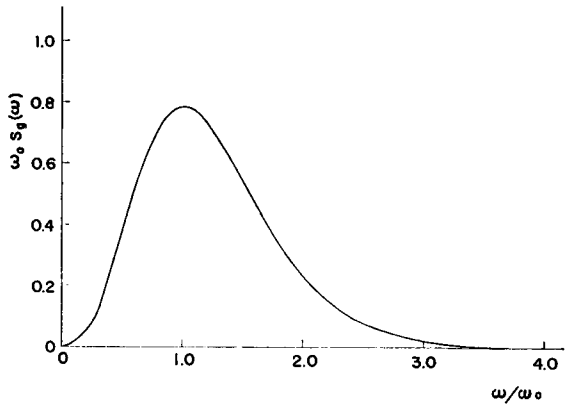

Fig. 5. Power Spectrum of $g(t)$.

$$\sigma_{g_1} = 1\,, \quad \sigma_{g_2} = \frac{\sqrt{30}}{4}\omega_0 \qquad \cdots\cdots\cdots\cdots(14)$$

If $N_{c\alpha}(t)\,dt$ denotes the probability that $x(t)$ will cross a positive threshold value α with positive slope or a negative value $-\alpha$ with negative slope in the interval $(t,\ t+dt)$, then we have[5]

$$N_{c\alpha}(t) = \int_{-\infty}^{0} |\dot{x}|\,\phi_j(-\alpha,\ \dot{x};\ t)\,d\dot{x} + \int_{0}^{\infty} \dot{x}\phi_j(\alpha,\ \dot{x};\ t)\,d\dot{x} \qquad \cdots\cdots\cdots\cdots(15)$$

For the Gaussian distribution, Eq. (15) yields

$$N_{c\alpha}(t) = \frac{\sigma_2}{\sigma_1}\exp\left\{-\frac{1}{2}\left(\frac{\alpha}{\sigma_1}\right)^2\right\}\left[\frac{\sqrt{1-\rho_{12}^2}}{\pi}\exp\left(-\kappa^2\right) + \frac{\rho_{12}}{\sqrt{2\pi}}\frac{\alpha}{\sigma_1}\left\{1+\mathrm{erf}\,(\kappa)\right\}\right] \qquad \cdots\cdots\cdots\cdots(16)$$

where

$$\kappa = \frac{\rho_{12}}{\sqrt{2(1-\rho_{12}^2)}}\frac{\alpha}{\sigma_1}$$

and erf (x) is the error function.

The same discussions can be made for the earthquake velocity $v(t)$. From Eq. (4), we set

$$v(t) = \beta f(t;\ \tau)\int_{-\infty}^{t} g(t)\,dt \qquad \cdots\cdots\cdots\cdots(17)$$

The probability densities corresponding to Eqs. (7) and (8) are obtained as

$$\phi(v;\ t) = \frac{1}{\sqrt{2\pi}\,\sigma_0}\exp\left\{-\frac{1}{2}\left(\frac{v}{\sigma_0}\right)^2\right\} \qquad \cdots\cdots\cdots\cdots(18)$$

$$\phi_j(v, \dot{v}; t) = \frac{1}{2\pi\sigma_0\bar{\sigma}_1\sqrt{1-\rho_{01}^2}} \exp\left[-\frac{1}{2(1-\rho_{01}^2)}\left\{\left(\frac{v}{\sigma_0}\right)^2 - 2\rho_{01}\left(\frac{v}{\sigma_0}\right)\left(\frac{\dot{v}}{\bar{\sigma}_1}\right)+\left(\frac{\dot{v}}{\bar{\sigma}_1}\right)^2\right\}\right] \quad \cdots\cdots(19)$$

where

$$\left.\begin{aligned} \sigma_0 = \sigma_0(t) &= \left\{\mathrm{E}[v^2(t)]\right\}^{1/2} = \beta\sigma_{g_0} f(t;\tau) \\ \bar{\sigma}_1 = \bar{\sigma}_1(t) &= \left\{\mathrm{E}[\dot{v}^2(t)]\right\}^{1/2} = \beta\left\{\sigma_{g_0}^2 \dot{f}^2(t;\tau) + \sigma_{g_1}^2 f^2(t;\tau)\right\}^{1/2} \\ \rho_{01} = \rho_{01}(t) &= \frac{\mathrm{E}[v(t)\dot{v}(t)]}{\sigma_0\bar{\sigma}_1} = \beta^2\frac{\sigma_{g_0}^2}{\sigma_0\bar{\sigma}_1} f(t;\tau)\dot{f}(t;\tau) \end{aligned}\right\} \quad \cdots\cdots(20)$$

for which σ_{g_1} is given in Eq. (10) and σ_{g_0} is computed from

$$\sigma_{g_0}^2 = \mathrm{E}\left[\left\{\int_{-\infty}^{t} g(t)\,dt\right\}^2\right] = \int_0^\infty \frac{S_g(\omega)}{\omega^2}\,d\omega \quad \cdots\cdots(21)$$

On substitution from Eq. (12) to Eq. (21), we obtain

$$\sigma_{g_0} = \frac{2}{\sqrt{3}\,\omega_0} \quad \cdots\cdots(22)$$

The quantity $N_{cv_m}(t)$ similar to $N_{c\alpha}(t)$ in Eq. (15) is obtained by replacing $\dot{x}$, $\phi_j(-\alpha, \dot{x}; t)$ and $\phi_j(\alpha, \dot{x}; t)$ by $\dot{v}$, $\phi_j(-v_m, \dot{v}; t)$ and $\phi_j(v_m, \dot{v}; t)$, respectively, in which $\pm v_m$ are the threshold values for $v(t)$ corresponding to $\pm\alpha$. Likewise, Eq. (16) applies to the case of velocity if we substitute σ_0, $\bar{\sigma}_1$, ρ_{01}, and v_m for σ_1, σ_2, ρ_{12}, and α, respectively.

For the interval $0 \leqq t \leqq \tau$ in which $x(t)$ is stationary, Eqs. (9) and (16), by virtue of Eq. (14), are greatly simplified:

$$\sigma_1 = \beta\,, \quad \sigma_2 = \frac{\sqrt{30}}{4}\beta\omega_0 = 2.7386\frac{\pi\beta}{T_0}\,, \quad \rho_{12} = 0 \quad \cdots\cdots(23)$$

where $T_0 = 2\pi/\omega_0$: predominant period, and

$$N_{c\alpha}(t) = N_{c\alpha} = \frac{2.7386}{T_0}\exp\left\{-\frac{1}{2}\left(\frac{\alpha}{\sigma_1}\right)^2\right\} \quad \cdots\cdots(24)$$

In the same manner, the quantities related to the velocity $v(t)$ are simplified to assume the following form:

$$\sigma_0 = \frac{2\beta}{\sqrt{3}\,\omega_0} = \frac{\beta T_0}{\sqrt{3}\,\pi}\,, \quad \bar{\sigma}_1 = \sigma_1 = \beta\,, \quad \rho_{01} = 0 \quad \cdots\cdots(25)$$

and

$$N_{cv_m}(t) = N_{cv_m} = \frac{\sqrt{3}}{T_0} \exp\left\{-\frac{1}{2}\left(\frac{v_m}{\sigma_0}\right)^2\right\} \qquad \cdots\cdots(26)$$

In the vicinity of $t=-0$ and $t=\tau+0$, $\dot{f}(t;\tau)$ involves the impulse function, the effects of which must be considered in the next chapter.

3. Probability Distribution of the Maximum Ground Motion in a Single Earthquake

(1) Basic Analysis

The derivation of the probability distribution of the maximum ground motion involved in a single earthquake for the statistical model proposed in the previous chapter can be reduced to the first-occurrence problem for two-sided barriers in random processes. First, let α denote the maximum ground acceleration in a single earthquake described by Eq. (4). Then the probability distribution $\Phi_s(\alpha)$ of α is represented by

$$\begin{aligned}\Phi_s(\alpha) &= \mathrm{P}[\max|x(t)| \leqq \alpha;\ 0 \leqq t \leqq \tau] \\ &= \mathrm{P}[|x(0)| \leqq \alpha]\left\{1-\int_0^\tau p_0(\alpha;\ t)\,dt\right\} \qquad \cdots\cdots(27)\end{aligned}$$

where $p_0(\alpha;\ t)$ is the first-occurrence density defined by

$$p_0(\alpha;\ t)dt = \mathrm{P}\left[\left\{(\max|x(\bar{t})| \leqq \alpha;\ 0 \leqq \bar{t} \leqq t) \cap (|x(t+dt)| > \alpha)\right\}\middle| |x(0)| \leqq \alpha\right] \qquad \cdots\cdots(28)$$

Here $\mathrm{P}[R_1|R_2]$ is the conditional probability of an event R_1 on the hypothesis of the event R_0. Under the Gaussian assumption, $\mathrm{P}[|x(0)| \leqq \alpha]$ is given by

$$\mathrm{P}[|x(0)| \leqq \alpha] = \mathrm{erf}\left\{\frac{\alpha}{\sqrt{2}\,\sigma_1(0)}\right\} \qquad \cdots\cdots(29)$$

It is an extremely difficult task to find out the exact solution for $p_0(\alpha;\ t)$. However, its asymptotic behaviour for large α has been discussed by J. J. Coleman[6] and generalized by J. R. Rice and F. P. Beer.[7] Rice and Beer discussed the first-occurrence density for a one-sided barrier problem. On applying their results to our present two-sided barrier problem, we have

$$\int_0^\tau p_0(\alpha;\ t)\,dt \cong 1-\exp\left\{-\int_0^\tau N_{c\alpha}(t)\,dt\right\} \qquad \cdots\cdots(30)$$

where $N_{c\alpha}(t)$ is given in Eq. (15) or (16). Eq. (30) tends to the exact solution for small τ/T_0 or for such large α that the crossing of $x(t)=\pm\alpha$ occurs almost

independently of the previous crossing of the same level. Since we are dealing with processes stationary and Gaussian in the interval $0 \leqq t \leqq \tau$, Eqs. (23) and (24) apply. Thus with the aid of Eqs. (23), (24), (29) and (30), an approximation $\Psi_s(\alpha)$ to the probability distribution $\Phi_s(\alpha)$ in Eq. (27) is obtained as follows:

$$\Psi_s(\alpha) = \mathrm{erf}\left(\frac{\alpha}{\sqrt{2}\,\beta}\right) \exp\left[-2.7386\frac{\tau}{T_0}\exp\left\{-\frac{1}{2}\left(\frac{\alpha}{\beta}\right)^2\right\}\right] \quad \cdots\cdots\cdots(31)$$

If we set

$$\Psi_{sn}(\zeta) = \Psi_s(\alpha)\,, \quad \zeta = \frac{\alpha}{\sigma_1} = \frac{\alpha}{\beta} \quad \cdots\cdots\cdots\cdots(32)$$

then $\Psi_s(\alpha)$ is normalized as

$$\Psi_{sn}(\zeta) = \mathrm{erf}\left(\frac{\zeta}{\sqrt{2}}\right) \exp\left\{-2.7386\frac{\tau}{T_0}\exp\left(-\frac{\zeta^2}{2}\right)\right\} \quad \cdots\cdots\cdots\cdots(33)$$

In the same manner, we obtain an approximation $\tilde{\Psi}_s(v_m)$ to the probability distribution $\tilde{\Phi}_s(v_m)$ of the maximum velocity v_m as

$$\tilde{\Psi}_s(v_m) = \mathrm{erf}\left(\frac{\sqrt{3}\,\pi}{\sqrt{2}\,\beta T_0}v_m\right) \exp\left[-\sqrt{3}\,\frac{\tau}{T_0}\exp\left\{-\frac{1}{2}\left(\frac{\sqrt{3}\,\pi}{\beta T_0}v_m\right)^2\right\}\right] \quad \cdots(34)$$

and its normalized form as

$$\tilde{\Psi}_{sn}(\eta) = \mathrm{erf}\left(\frac{\eta}{\sqrt{2}}\right) \exp\left\{-\sqrt{3}\,\frac{\tau}{T_0}\exp\left(-\frac{\eta^2}{2}\right)\right\} \quad \cdots\cdots\cdots\cdots(35)$$

where

$$\eta = \frac{v_m}{\sigma_0} = \frac{\sqrt{3}\,\pi}{\beta T_0}v_m \quad \cdots\cdots\cdots\cdots(36)$$

Fig. 6 shows $\Psi_{sn}(\zeta)$ and $\tilde{\Psi}_{sn}(\eta)$ for various values of τ/T_0. We see that the non-excess probability at relatively lower levels of ζ and η almost vanishes as τ/T_0 increases. We could, therefore, expect that Eqs. (28)$\sim$(36) will furnish good approximations to the exact solutions $\Phi_s(\alpha)$ and $\tilde{\Phi}_s(v_m)$ if τ/T_0 is properly large.

Next, the accuracy of these formulae is examined in two ways; i.e., they are compared with 1) the theoretical upper and lower bounds and with 2) the result of a numerical simulation. The former method would serve for a check of the approximation error in lower and higher ranges of α and v_m, and the latter, in an intermediate range. It suffices to make these tests for the lower limit of τ/T_0, since the larger τ/T_0 is the more accurate the approximation becomes. In most major earthquakes τ/T_0 would fall into the range of some 10$\sim$100. Hence in the present test of accuracy, τ/T_0 is taken as 10 and 30; the latter value is used for the application in the next chapter.

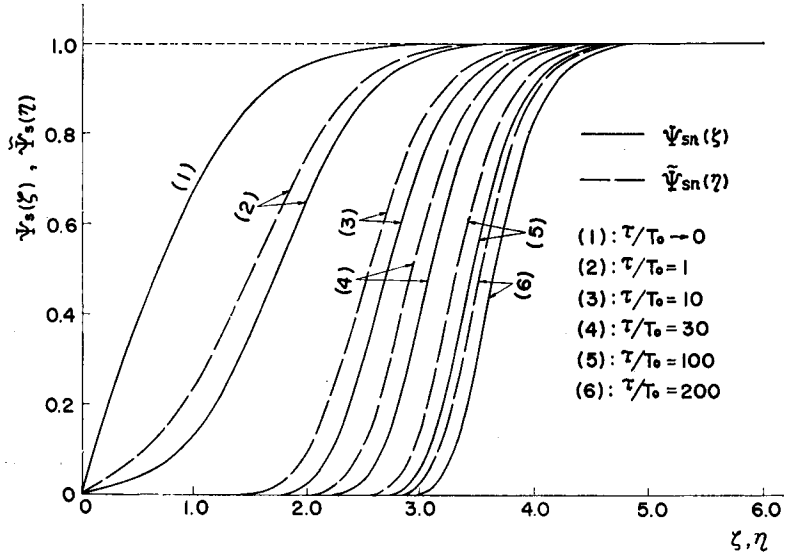

Fig. 6. Approximate Probability Distribution of the Maximum Acceleration in a Single Earthquake.

A method for determining the lower and upper bounds of the probability of excess in a random process has been presented by M. Shinozuka.[8] In what follows, his method is improved on so as to give closer bounds to the real value. First, we discuss the lower bound of $\Phi_s(\alpha)$.

Let t' and t'' be instants such that

$$-\infty < t' \leqq t, \quad t < t'' \leqq t+dt$$

Then the differential with respect to t of the probability that $\max|x(t')|$ will be in excess of α is given[8] by

$$dP[\max|x(t')| > \alpha] = P[\{\max|x(t')| \leqq \alpha\} \cap \{\max|x(t'')| > \alpha\}] \quad \cdots(37)$$

For the instants τ_k defined by

$$-\infty < \tau_1 < \tau_2 < \cdots < \tau_{n+1} = t$$

in which $n=n(t)$ is also a function t, we have

$$P[\{\max|x(t')| \leqq \alpha\} \cap \{\max|x(t'')| > \alpha\}]$$
$$< P[\{\bigcap_{k=1}^{n(t)+1} |x(\tau_k)| \leqq \alpha\} \cap \{\max|x(t'')| > \alpha\}] \quad \cdots\cdots\cdots(38)$$

But if we choose $\tau_1, \cdots, \tau_n$ so that $x(t)=x(\tau_{n+1})$ is independent of $x(\tau_1)$, $x(\tau_2)$, $\cdots$, $x(\tau_n)$, then obviously

$$\begin{aligned}
&P[\{\bigcap_{k=1}^{n(t)+1}|x(\tau_k)|\leqq\alpha\}\cap\{\max|x(t'')|>\alpha\}]\\
&\quad=P[\bigcap_{k=1}^{n(t)}|x(\tau_k)|\leqq\alpha]\cdot P[\{|x(t)|\leqq\alpha\}\cap\{\max|x(t'')|>\alpha\}]\\
&\quad=P[\bigcap_{k=1}^{n(t)}|x(\tau_k)|\leqq\alpha]\cdot N_{c\alpha}(t)\,dt \qquad\cdots\cdots\cdots\cdots(39)
\end{aligned}$$

Thus we obtain

$$dP[\max|x(t')|>\alpha]<P[\bigcap_{k=1}^{n(t)}|x(\tau_k)|\leqq\alpha]\cdot N_{c\alpha}(t)\,dt$$

and hence

$$P[\max|x(t)|>\alpha]<\int_{-\infty}^{\infty}P[\bigcap_{k=1}^{n(t)}|x(\tau_k)|\leqq\alpha]\cdot N_{c\alpha}(t)\,dt \qquad\cdots\cdots\cdots\cdots(40)$$

And by virtue of the fact that $\Phi_s(\alpha)$ can also be written as

$$\Phi_s(\alpha)=1-P[\max|x(t)|>\alpha]$$

the lower bound $\Phi_{sl}(\alpha)$ of $\Phi_s(\alpha)$ is represented in the following form:

$$\Phi_{sl}(\alpha)=1-\int_{-\infty}^{\infty}P[\bigcap_{k=1}^{n(t)}|x(\tau_k)|\leqq\alpha]\cdot N_{c\alpha}(t)\,dt<\Phi_s(\alpha) \qquad\cdots\cdots\cdots\cdots(41)$$

In the present analysis the τ_k are chosen as illustrated in Fig. 7. In this figure, τ_0 is the value of τ at which $R(\tau)$ first crosses the τ-axis, and τ_c is the correlation time for which $R(\tau)$ becomes so small that $g(t)$ and $g(t+\tau_a)$ can be treated as independent for any τ_a such that $\tau_a\geqq\tau_c$. It is noted that $n(t)$ must

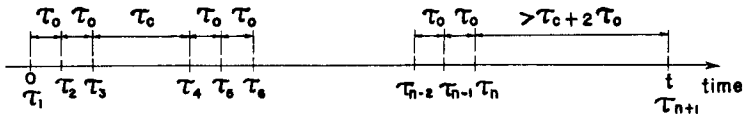

Fig. 7. Illustration of the Instants τ_k.

be integral times three. The value of $(t-\tau_n)$ is taken greater than $\tau_c+2\tau_0$. Then $x(t)$ is independent of $x(\tau_1)$, $x(\tau_2)$, $\cdots$, $x(\tau_n)$, and any of $x(\tau_{3p-2})$, $x(\tau_{3p-1})$, $x(\tau_{3p})$ are also independent of $x(\tau_{3s-2})$, $x(\tau_{3s-1})$, $x(\tau_{3s})$, $(p, s=1, 2, \cdots, n(t)/3; p\neq s)$. It is further noted that $x(\tau_{3p-1})$ is independent of $x(\tau_{3p-2})$ and $x(\tau_{3p})$, but there is a correlation between $x(\tau_{3p-2})$ and $x(\tau_{3p})$. Thus we have

$$\begin{aligned}
&P[\bigcap_{k=1}^{n(t)}|x(\tau_k)|\leqq\alpha]=\prod_{p=1}^{n(t)/3}P[\bigcap_{j=-2}^{0}|x(\tau_{3p+j})|\leqq\alpha]\\
&\quad=\prod_{p=1}^{n(t)/3}\{P[|x(\tau_{3p-1})|\leqq\alpha]\cdot P[|x(\tau_{3p-2})|\leqq\alpha\cap|x(\tau_{3p})|\leqq\alpha]\}\\
&\qquad\qquad\qquad\qquad\qquad\qquad\qquad\qquad\qquad\qquad\cdots\cdots\cdots\cdots(42)
\end{aligned}$$

which yields, for the stationary Gaussian process,

$$\begin{aligned} &P[\bigcap_{k=1}^{n(t)} |x(\tau_k)| \leqq \alpha] \\ &\quad = \{P[|x(\tau_{3p-1})| \leqq \alpha] \cdot P[|x(\tau_{3p-2})| \leqq \alpha \cap |x(\tau_{3p})| \leqq \alpha]\}^{n(t)/3} \\ &\quad = \{p_s(\alpha)\}^{n(t)/3} \end{aligned} \quad \cdots\cdots\cdots\cdots (43)$$

where

$$\begin{aligned} p_s(\alpha) = \operatorname{erf}\left(\frac{\alpha}{\sqrt{2}\beta}\right) \cdot \frac{1}{\sqrt{2\pi}} \int_0^{\alpha/\beta} \exp\left(-\frac{\xi^2}{2}\right) \Bigg[\operatorname{erf}\left\{\frac{1}{\nu}\left(\frac{\alpha}{\beta} + R(2\tau_0)\cdot\xi\right)\right\} \\ + \operatorname{erf}\left\{\frac{1}{\nu}\left(\frac{\alpha}{\beta} - R(2\tau_0)\cdot\xi\right)\right\} \Bigg] d\xi \end{aligned} \quad \cdots\cdots\cdots\cdots (44)$$

$$\nu = \sqrt{2(1-\{R(2\tau_0)\}^2)}$$

As we see from Eqs. (6), (9) and (16), the impulse function is involved in the integration of Eq. (41), which is carried out first by considering an approximating polygonal function in a small interval and letting the length of this interval tend to zero after integration. By such a process, the lower bound $\Phi_{sl}(\alpha)$ is obtained from Eq. (41) as

$$\Phi_{sl}(\alpha) = \operatorname{erf}\left(\frac{\alpha}{\sqrt{2}\beta}\right) - 2.7386 \frac{\tau}{KT_0} \frac{1-\{p_s(\alpha)\}^K}{1-p_s(\alpha)} \exp\left\{-\frac{1}{2}\left(\frac{\alpha}{\beta}\right)^2\right\} \quad \cdots\cdots\cdots\cdots (45)$$

where

$$K = n(\tau)/3$$

The upper bound $\Phi_{su}(\alpha)$ of $\Phi_s(\alpha)$ is obviously given by

$$\Phi_{su}(\alpha) = P[\bigcap_{k=1}^{n(\tilde{\tau})} |x(\tau_k)| \leqq \alpha] = \{p_s(\alpha)\}^{K+1} > \Phi_s(\alpha) \quad \cdots\cdots\cdots\cdots (46)$$

where

$$\tilde{\tau} = \tau + \tau_c + 2\tau_0$$

The normalized form of Eqs. (45) and (46) analogous to Eq. (33) is obtained, respectively, as follows:

$$\Phi_{sln}(\zeta) = \operatorname{erf}\left(\frac{\zeta}{\sqrt{2}}\right) - 2.7386 \frac{\tau}{KT_0} \frac{1-\{p_{sn}(\zeta)\}^K}{1-p_{sn}(\zeta)} \exp\left(-\frac{\zeta^2}{2}\right) \quad \cdots\cdots (47)$$

$$\Phi_{sun}(\zeta) = \{p_{sn}(\zeta)\}^{K+1} \quad \cdots\cdots\cdots\cdots (48)$$

where

$$\zeta = \frac{\alpha}{\beta}, \quad p_{sn}(\zeta) = p_{sn}\left(\frac{\alpha}{\beta}\right) = p_s(\alpha)$$

From Eq. (13), we obtain

$$\tau_0/T_0 = 0.2068\,, \quad R(2\tau_0) = -0.4005$$

and it would suffice to take the correlation time τ_c as

$$\tau_c/T_0 = 3.5$$

Using these data, the lower and upper bounds of $\Phi_s(\alpha)$ can be computed for any τ/T_0 with the aid of Eqs. (45) and (46) or of Eqs. (47) and (48), examples of which are shown in Fig. 8 for $\tau/T_0=10$ and 30 in comparison with $\Psi_{sn}(\zeta)$ in Eq. (33). It is observed that $\Phi_{sln}(\zeta)$ and $\Psi_{sn}(\zeta)$ almost coincide in the range $\zeta>3.1$ for $\tau/T_0=10$ and in $\zeta>3.5$ for $\tau/T_0=30$ which correspond to the non-excess probability of about 0.8. From the statistical meaning of $\Phi_{sln}(\zeta)$ and $\Psi_{sn}(\zeta)$, it is reasonable to assert that they both will furnish good approximations to $\Phi_s(\alpha)$ in higher range of ζ. Thus it could be stated that the approximation by Eq. (33) is good enough at least for the non-excess probability level higher than some 0.8. For the lower range of ζ, the question how well $\Psi_{sn}(\zeta)$ approximates the real distribution does not pose a serious problem, since it almost vanishes for such ζ, and indeed so does the upper bound $\Phi_{sun}(\zeta)$ as shown in Fig. 8.

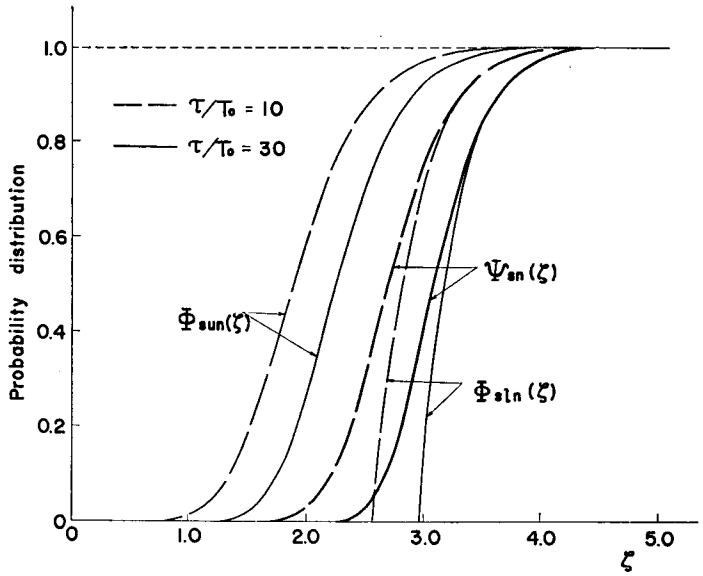

Fig. 8. Upper and Lower Bounds of the Probability Distribution of the Maximum Acceleration in a Single Earthquake.

The upper and lower bounds of the probability distribution $\Phi_s(v_m)$ of the maximum velocity can be discussed in exactly the same manner, for which case there have been obtained similar results.

Finally, the numerical simulation was made on a digital computer, in which 219 sample accelerograms were generated for $\tau/T_0=10$ and 73 of them for $\tau/T_0=30$. The earthquake velocity was examined for 174 and 58 sample earthquakes for $\tau/T_0=10$ and 30, respectively. The method of simulation of artificial earthquakes presented by one of the authors, K. Toki and T. Akiyoshi[9] has been

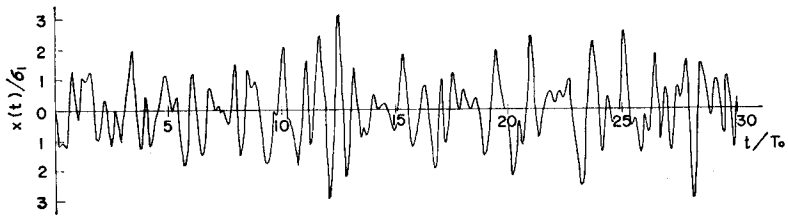

Fig. 9. Simulated Sample Accelerogram ($\tau/T_0=30$).

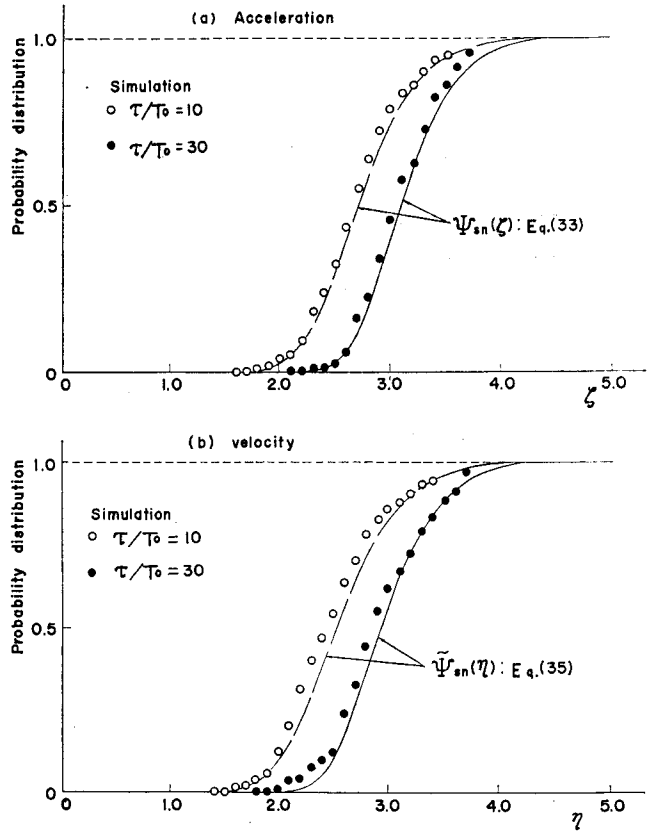

Fig. 10. Experimental Distributions of the Maximum Ground Motion in a Single Earthquake.

used. Fig. 9 shows an example of the sample accelerogram for $\tau/T_0=30$. Figs. 10(a) and (b) are the plots of the experimental distribution functions compared with $\Psi_{sn}(\zeta)$ and $\tilde{\Psi}_{sn}(\eta)$, respectively. In both cases the experimental and the theoretical values are in fairly good agreement.

From these discussions it would be appropriate to conclude that Eqs. (31) ~(36) provide good approximations to the probability distribution of the maximum ground motion in a single earthquake.

(2) The Intensity Parameter β

The parameter β in Eq. (4) is to be related to the intensity of earthquakes. In this study, β_I which denotes the value of β for the earthquakes of intensity I is determined so that the mean value of the maximum ground acceleration in a single earthquake of intensity I may equal the earthquake acceleration α_I obtained for the same intensity from the empirical formula proposed by seismologists; i.e., we set

$$\mathrm{E}[\alpha] = \alpha_I \qquad \cdots\cdots\cdots\cdots(49)$$

The mean value of a random variable z in terms of its probability distribution $\Phi(z)$ is represented by

$$\begin{aligned}\mathrm{E}[z] &= \int_{-\infty}^{\infty} z\,d\Phi(z) = \lim_{G\to\infty}\int_{-G}^{G} z\,d\Phi(z)\\ &= \lim_{G\to\infty}\left[\int_0^G \{\Phi(G)-\Phi(z)\}\,dz+\int_{-G}^{0}\{\Phi(-G)-\Phi(z)\}\,dz\right.\\ &= \int_0^{\infty}\{1-\Phi(z)\}\,dz-\int_{-\infty}^{0}\Phi(z)\,dz \qquad \cdots\cdots\cdots\cdots(50)\end{aligned}$$

Since the maximum acceleration α takes on only non-negative values, the last term of Eq. (50) applied to the present analysis vanishes, and Eq. (49) assumes the form

$$\mathrm{E}[\alpha] = \int_0^{\infty}\{1-\Phi_s(\alpha)\}\,d\alpha = \alpha_I \qquad \cdots\cdots\cdots\cdots(51)$$

If we use the approximate distribution functions $\Psi_s(\alpha)$ and $\Psi_{sn}(\zeta)$, we have

$$\mathrm{E}[\alpha] \cong \int_0^{\infty}\{1-\Psi_s(\alpha)\}\,d\alpha = \beta_I\int_0^{\infty}\{1-\Psi_{sn}(\zeta)\}\,d\zeta = \alpha_I$$

Hence β_I is obtained as

$$\beta_I = \alpha_I \Big/ \int_0^{\infty}\{1-\Psi_{sn}(\zeta)\}\,d\zeta \qquad \cdots\cdots\cdots\cdots(52)$$

As mentioned in the previous chapter, β_I^2 represents the variance of the stationary part of the accelerogram. Hence β_I serves as a direct measure of the earthquake intensity in the structural response analysis in which the structure is subjected to an ensemble of random earthquakes with a certain assigned r.m.s. intensity. Fig. 11 is a plot of β_I/α_I versus τ/T_0. It is noted that β_I does not change greatly in the range $\tau/T_0=10\sim100$ which is of interest to us. This fact simplifies the problem since we can assert that the duration of the earthquake has little effect upon the mean value of the maximum ground motion.

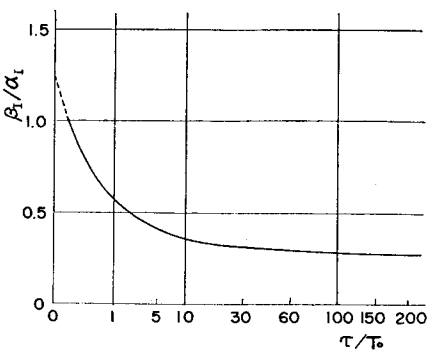

Fig. 11. The Intensity Parameter β_I (cubic-root scale for abscissa).

The empirical formula by which to determine α_I is discussed in the next section.

(3) Determination of α_I

The intensity parameter β_I (or β) is affected directly by what formula we use for the determination of α_I. The study by Kawasumi[1] is based on his own formula of the form

$$\alpha_I = 0.45\times10^{0.5I}\ (\mathrm{cm/sec^2})\ ,\quad I\text{: JMA scale} \qquad \cdots\cdots\cdots\cdots(53)$$

from which we have

$$\alpha_{\mathrm{V}} = 142\ (\mathrm{cm/sec^2})\ ,\quad \alpha_{\mathrm{VI}} = 450\ (\mathrm{cm/sec^2})\ ,\quad \alpha_{\mathrm{VII}} = 1420\ (\mathrm{cm/sec^2}) \qquad \cdots\cdots\cdots\cdots(54)$$

With this formula, however, the mean value of the future maximum earthquake acceleration for a locality which has experienced earthquakes of intensity VII becomes unrealistically large as we shall see later, mainly due to such a large value for α_{VII}. Hence in this section, we shall search for another method for determining α_I.

K. Kanai[10] recently proposed a new formula with an account for the predominant period T_0 on the basis of the data for $I_{\mathrm{MM}}=6\sim8$, (I_{MM}: modified Mercalli intensity scale):

$$\alpha_{I_{\mathrm{MM}}} = 0.62\ T_0^{-1.316}\ 10^{0.238 I_{\mathrm{MM}}}\ (\mathrm{cm/sec^2})\ ,\quad T_0\text{: in sec} \qquad \cdots\cdots\cdots\cdots(55)$$

For $I_{\mathrm{MM}}=8$; i.e., for $I=\mathrm{V}$ in the JMA scale, we have

$$\alpha_V = 50\ T_0^{-1.316}\ (\mathrm{cm/sec^2}) \qquad \cdots\cdots\cdots\cdots(56)$$

For higher intensities, the values of acceleration proposed by JMA[11] shall be refered to. The middle value of the upper and lower bounds of the JMA acceleration for I=V is given as 170 cm/sec^2, which corresponds to T_0=0.395≅0.4 sec in Eq. (56). We assume that the JMA values for higher I correspond to T_0=0.4 sec as well and that in this range of I the earthquake acceleration is also proportional to $T_0^{-1.316}$. The middle value of the JMA acceleration for I=VI is 320 cm/sec^2. Hence we have

$$\alpha_{VI} = 320\left(\frac{T_0}{0.4}\right)^{-1.316} = 96\ T_0^{-1.316}\ (\mathrm{cm/sec^2}) \qquad \cdots\cdots\cdots\cdots(56')$$

For I=VII, JMA acceleration gives only the lower bound. On the other hand, the acceleration for I=V varies as 80∼250 cm/sec^2 for which the difference between the upper and lower bounds is 170 cm/sec^2. Likewise, the acceleration for I=VI varies as 250∼400 cm/sec^2 whose difference is 150 cm/sec^2. Thus the difference between the upper and lower bounds is approximately 150 cm/sec^2. Extrapolating this fact to I=VII, we assume that the acceleration for the intensity VII varies as 400∼550 cm/sec^2 and take the mean as 470 cm/sec^2. Applying the above procedure, we obtain

$$\alpha_{VII} = 470\left(\frac{T_0}{0.4}\right)^{-1.316} = 140\ T_0^{-1.316}\ (\mathrm{cm/sec^2}) \qquad \cdots\cdots\cdots\cdots(56'')$$

4. Probability Distribution of the Maximum Ground Motion at a Certain Locality in a Future Period

(1) Formal Representation

If the probability distribution of the maximum ground motion in a single earthquake discussed in the previous chapter is known, the probability distribution of the maximum earthquake ground motion to occur at a certain locality in a future period can be determined with the aid of the statistical model of occurrence of earthquakes proposed in **2**.(1).

Let α_f denote the maximum earthquake acceleration to occur in a future interval B_f of length S_f, and A_f denote its realized value. If $R_f(k_{I1}, k_{I2}, \cdots, k_{Im})$ represents the event that $k_{I1}, k_{I2}, \cdots, k_{Im}$ earthquakes of intensity $I_1, I_2, \cdots, I_m$, respectively, occur in B_f, then the conditional probability distribution $\Phi_c(\alpha_f | k_{I1}, k_{I2}, \cdots, k_{Im})$ of α_f on the hypothesis of $R_f(k_{I1}, k_{I2}, \cdots, k_{Im})$ is given by

$$\Phi_c(\alpha_f|k_{I1}, k_{I2},\cdots, k_{Im}) = \mathrm{P}[A_f \leqq \alpha_f|R_f(k_{I1}, k_{I2},\cdots, k_{Im})]$$
$$= \prod_{j=1}^{m} \{\Phi_s(\alpha_f; I_j)\}^{k_{Ij}} \quad \cdots\cdots\cdots\cdots(57)$$

where $\Phi_s(\alpha_f; I_j)$ is the value of $\Phi_s(\alpha_f)$ in which β_{Ij} is used for β.

But the probability of the event $R_f(k_{I1}, k_{I2},\cdots, k_{Im})$ is given by Eq. (3). Hence the probability of the event $\{A_f \leqq \alpha_f \cap R_f(k_{I1}, k_{I2},\cdots, k_{Im})\}$ is represented by

$$\mathrm{P}[A_f \leqq \alpha_f \cap R_f(k_{I1}, k_{I2},\cdots, k_{Im})]$$
$$= \Phi_c(\alpha_f|k_{I1}, k_{I2},\cdots, k_{Im})\, P_c(k_{I1}, k_{I2},\cdots, k_{Im})$$
$$= \prod_{j=1}^{m} [\{\Phi_s(\alpha_f; I_j)\}^{k_{Ij}} \mathrm{b}(k_{Ij}; n_{Ij}, P_f)] \quad \cdots\cdots\cdots\cdots(58)$$

The events $R_f(k_{I1}, k_{I2},\cdots, k_{Im})$ and $R_f(l_{I1}, l_{I2},\cdots, l_{Im})$ are exclusive if $\bigcup_{j=1}^{m} (k_{Ij} \neq l_{Ij})$ holds. Hence from a simple Boolean algebra, we can derive the probability distribution $\Phi_f(\alpha_f)$ of the maximum earthquake acceleration in the future interval B_f in the following form:

$$\Phi_f(\alpha_f) = \mathrm{P}[\bigcup_{k_{I1}=0}^{n_{I1}} \bigcup_{k_{I2}=0}^{n_{I2}} \cdots \bigcup_{k_{Im}=0}^{n_{Im}} \{A_f \leqq \alpha_f \cap R_f(k_{I1}, k_{I2},\cdots, k_{Im})\}]$$
$$= \sum_{k_{I1}=0}^{n_{I1}} \sum_{k_{I2}=0}^{n_{I2}} \cdots \sum_{k_{Im}=0}^{n_{Im}} \mathrm{P}[A_f \leqq \alpha_f \cap R_f(k_{I1}, k_{I2},\cdots, k_{Im})]$$
$$= \sum_{k_{I1}=0}^{n_{I1}} \sum_{k_{I2}=0}^{n_{I2}} \cdots \sum_{k_{Im}=0}^{n_{Im}} \{\prod_{j=1}^{m} [\{\Phi_s(\alpha_f; I_j)\}^{k_{Ij}} \mathrm{b}(k_{Ij}; n_{Ij}, P_f)]\} \quad \cdots(59)$$

Likewise, the approximate distribution function $\Psi_f(\alpha_f)$ of the future maximum acceleration is obtained as

$$\Psi_f(\alpha_f) = \sum_{k_{I1}=0}^{n_{I1}} \sum_{k_{I2}=0}^{n_{I2}} \cdots \sum_{k_{Im}=0}^{n_{Im}} \{\prod_{j=1}^{m} [\Psi_s(\alpha_f; I_j)\}^{k_{Ij}} \mathrm{b}(k_{Ij}; n_{Ij}, P_f)]\} \quad \cdots(60)$$

where $\Psi_s(\alpha_f; I_j)$ is the value of $\Psi_s(\alpha_f)$ in which β_{Ij} is used for β.

In the same manner, the approximate distribution function $\tilde{\Psi}_f(v_{mf})$ of the future maximum earthquake velocity v_{mf} is represented in the following form:

$$\tilde{\Psi}_f(v_{mf}) = \sum_{k_{I1}=0}^{n_{I1}} \sum_{k_{I2}=0}^{n_{I1}} \cdots \sum_{k_{Im}=0}^{n_{Im}} \{\prod_{j=1}^{m} [\{\tilde{\Psi}_s(v_{mf}; I_j)\}^{k_{Ij}} \mathrm{b}(k_{Ij}; n_{Ij}, P_f)]\} \quad \cdots\cdots\cdots\cdots(61)$$

where $\tilde{\Psi}_s(v_{mf}; I_j)$ is the value of $\tilde{\Psi}_s(v_{mf})$ in which β_{Ij} is used for β.

By virtue of Eq. (50), the mean values of α_f and v_{mf} are represented in terms,

respectively, of $\Psi_f(\alpha_f)$ and $\tilde{\Psi}_f(v_{mf})$ by

$$\left.\begin{aligned} \mathrm{E}[\alpha_f] &\cong \int_0^\infty \{1-\Psi_f(\alpha_f)\}\, d\alpha_f \\ \mathrm{E}[v_{mf}] &\cong \int_0^\infty \{1-\tilde{\Psi}_f(v_{mf})\}\, dv_{mf} \end{aligned}\right\} \quad \cdots\cdots\cdots\cdots(62)$$

(2) Data of Past Earthquakes Prepared for Numerical Application

In the present study, we deal with earthquakes of intensity V, VI, and VII. Earthquakes of lower intensities are neglected because of lack of data of such earthquakes in former times. This, however, will not greatly affect the result since the acceleration for lower intensities rapidly decreases and $\Phi_s(\alpha_f; I_j)$ for such an intensity tends to unity even for small α_f.

Every locality on the main islands of Japan are represented by grid points taken at every 30′ in latitude and longitude. The shock intensities felt at these grid points were computed by means of Kawasumi's method[1] for all earthquakes indicated in the list of past destructive earthquakes in the Chronological Table of Science, 1966 whose dates, locations and magnitudes are known.

From the statistical point of view, the length S_r of the interval B_r should be sufficiently large compared with S_f. However, S_r must not be so large that B_r stretches over the ages in which the accuracy of the data of past earthquakes greatly varies. In this study, we take $S_r=150$ years for Hokkaisdo and $S_r=200$ years for other districts. Thus the numbers of earthquakes N, N_r, n_{V}, n_{VI}, n_{VII} were obtained. Some basic data of these past earthquakes are shown in the Appendix.

(3) Effect of τ/T_0

In computing the probability distribution of the future maximum ground motion, we must assign some proper value for τ/T_0. We have seen in **3**.(2) that β_I, hence the expected value $\mathrm{E}[\zeta]$ of ζ also, does not change greatly with τ/T_0 in the range of our interest. This is also true when the shape of $\Psi_s(\alpha; I)$ is concerned. Fig. 12 shows $\Psi_s(\alpha; I)$ plotted against its expected value α_I, from which we see that the shapes of $\Psi_s(\alpha; I)$ are almost similar for $\tau/T_0=10\sim100$. Thus we have the prospect for the validity of fixing the value of τ/T_0.

The approximate probability distribution $\Psi_f(\alpha_f)$ of the future maximum acceleration in Tokyo and Kyoto computed from Eq. (60) for the seismic data discussed in the previous section is shown in Fig. 13 for $T_0=0.5$ sec, $S_f=75$ years and various values of τ/T_0. For the determination of α_I, Eqs. (56)$\sim$(56″) have been used. Variation of $\Psi_f(\alpha_f)$ for different τ/T_0 would be small enough for engineering purposes. The expected value $\mathrm{E}[\alpha_f]$ computed from these distribu-

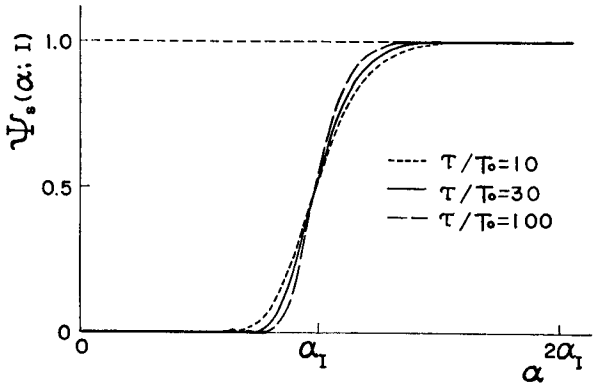

Fig. 12. Approximate Probability Distribution of the Maximum Acceleration in a Single Earthquake in Terms of Its Expected Value.

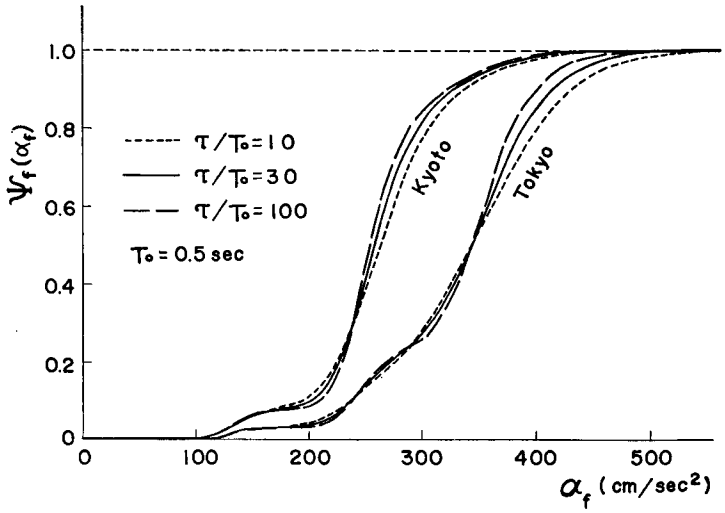

Fig. 13. Probability Distribution of the Maximum Earthquake Acceleration to Occur in 75 Years.

tion functions with the aid of Eq. (62) also varies in a small range; 328~336 cm/sec² for Tokyo and 255~262 cm/sec² for Kyoto. In what follows, we use $\tau/T_0=30$ which gives nearly the middle value of β_I between those for $\tau/T_0=10$ and $\tau/T_0=100$.

(4) Seismic Maps

The probability distributions $\Psi_f(\alpha_f)$ and $\tilde{\Psi}_f(v_{mf})$ of the future maximum ground motions and their expected values $E[\alpha_f]$ and $E[v_{mf}]$ were computed for all grid points covering Japan. The length of the future interval B_f was taken as

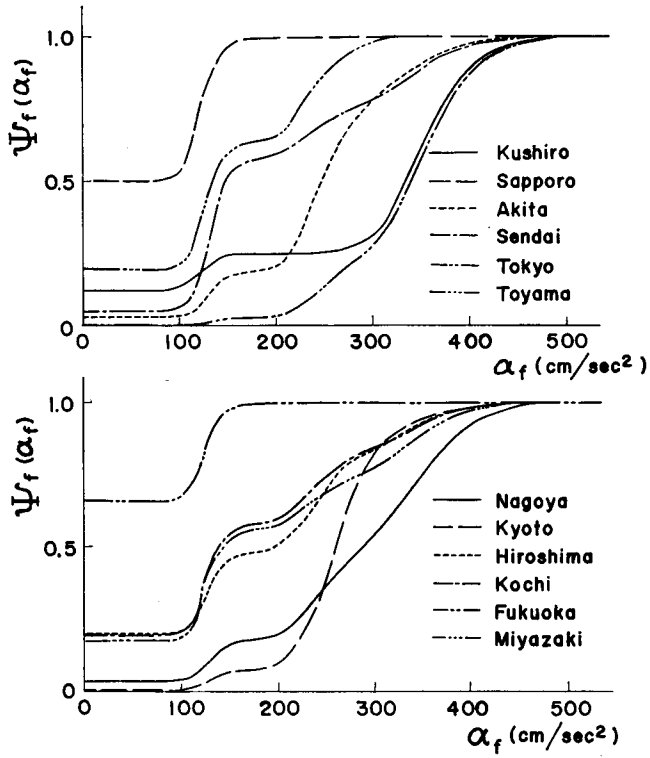

Fig. 14. Probability Distribution of the Maximum Earthquake Acceleration to Occur in 75 Years (T_0=0.5 sec, τ/T_0=30).

Table 1. Expected Value of the Maximum Earthquake Acceleration to Occur in 75 Years (T_0=0.5 sec, τ/T_0=30).

locality	E(α_f) (cm/sec^2)	locality	E(α_f) (cm/sec^2)
Kushiro	285	Nagoya	275
Sapporo	70	Kyoto	258
Akita	244	Hiroshima	183
Sendai	198	Kochi	172
Tokyo	332	Fukuoka	52
Toyama	147	Miyazaki	184

S_f=75 years. Some examples of $\Psi_f(\alpha_f)$ are shown in Fig. 14 and the corresponding expected values are indicated in Table 1. Eqs. (56)$\sim$(56″) have been used for the determination of α_I throughout this section. The finite value of $\Psi_f(0)$ results from casting earthquakes of lower intensities away, and it represents the probability that no earthquake of intensity higher than V will occur in the interval B_f. It is also noted that the shape of $\Psi_f(\alpha_f)$ varies greatly with localities.

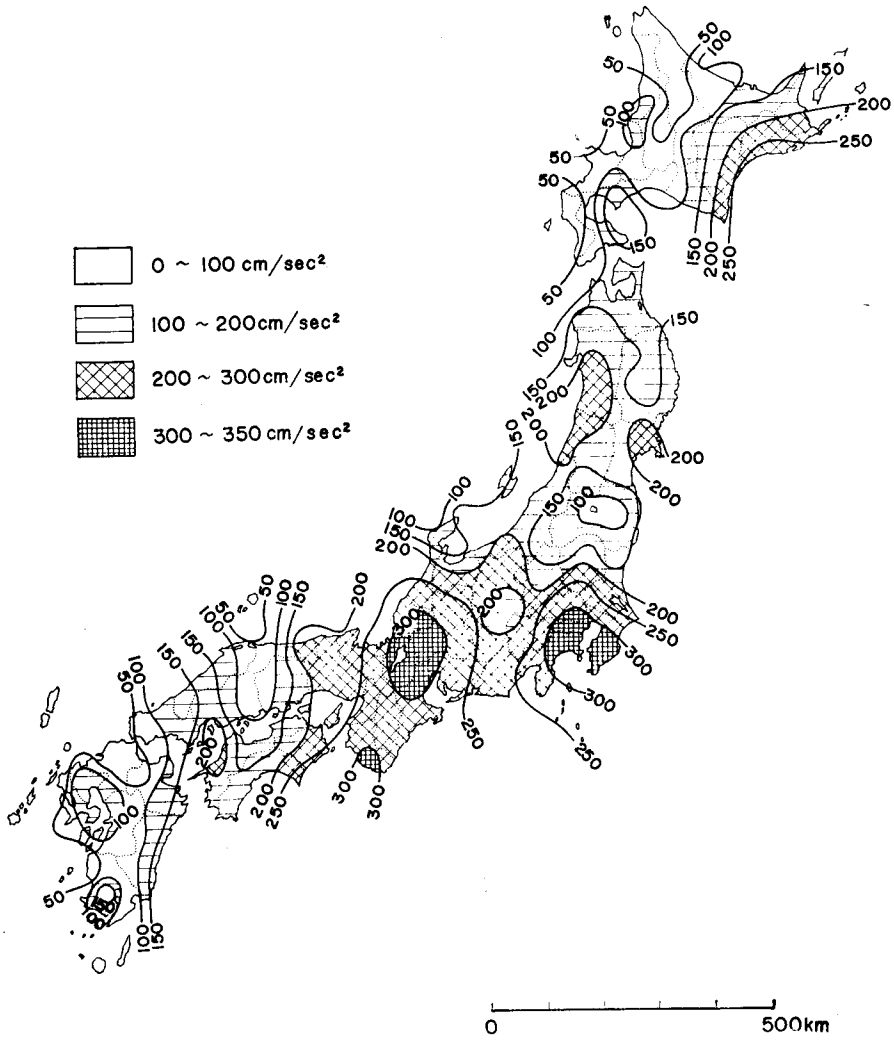

Fig. 15 Seismic Map for the Expected Value of the Maximum Earthquake Acceleration in 75 Years (T_0=0.5 sec, τ/T_0=30; Eqs. (56)~(56′) are used).

For example, in spite of the fact that $E[\alpha_f]$ for Kyoto is larger than that for Miyazaki, the value of α_f corresponding to the non-excess probability of 90% for Miyazaki is larger than that for Kyoto. Thus it is impossible to find out some standard shape for $\Psi_f(\alpha_f)$, so that when a precise probabilistic judgment must be made for α_f reference should be made not only to the expected value $E[\alpha_f]$ but also to the distribution function $\Psi_f(\alpha_f)$ particular to each locality. With this fact in mind, there is no doubt that the expected value $E[\alpha_f]$ is a direct measure of the future earthquake danger. Fig. 15 is a seismic map showing the distribution of

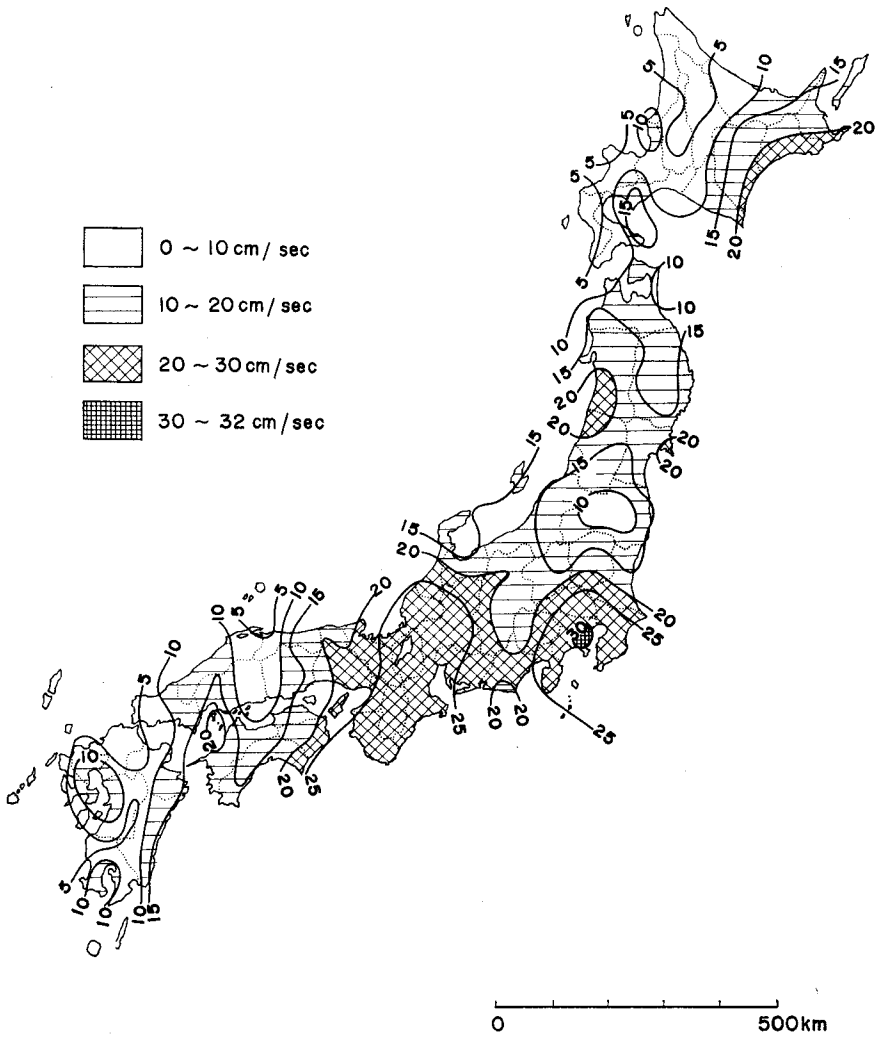

Fig. 16. Seismic Map for the Expected Value of the Maximum Earthquake Velocity in 75 Years (T_0=0.5 sec, τ/T_0=30; Eqs. (56)~(56″) are used).

$E[\alpha_f]$ throughout the main islands of Japan. Fig. 16 is the seismic map for the velocity $E[v_{mf}]$.

All discussions in this section have been made for the predominant period of 0.5 sec. Hence, when earthquakes with other predominant period T_0 is in question, all values for α_f and $E[\alpha_f]$ in this section must be multipled by $(T_0/0.5)^{-1.316}$, and v_{mf} and $E[v_{mf}]$, by $(T_0/0.5)^{-0.316}$; in both cases T_0 is given in sec.

(5) Comparison with the Seismic Map Prepared by H. Kawasumi

Our interest in this section is to compare the result of the present analysis with

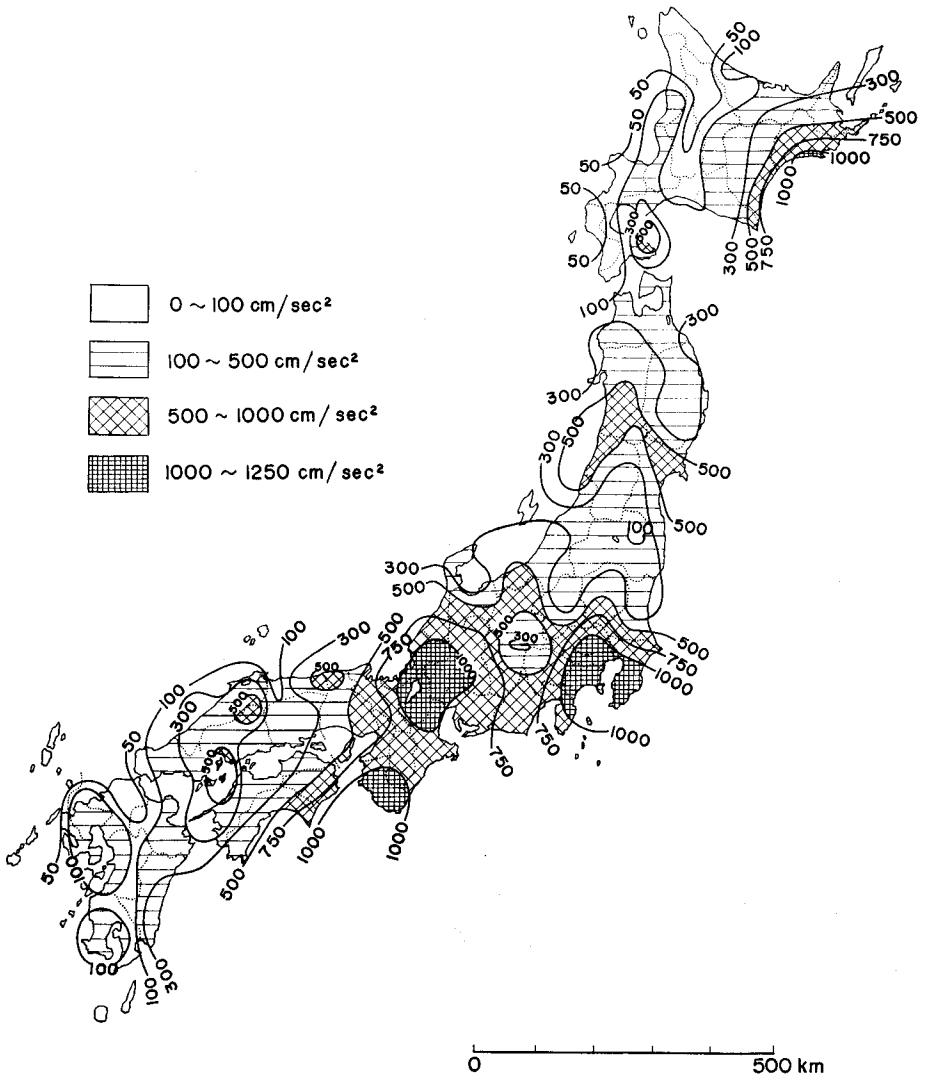

Fig. 17. Seismic Map for the Expected Value of the Maximum Earthquake Acceleration in 75 Years ($\tau/T_0=30$; Eq. (53) is used).

the seismic map showing the distribution of the expected values of the future maximum earthquake acceleration prepared by H. Kawasumi[1]. Fig. 17 is a seismic map same as Fig. 15 except that Eq. (53) has been used to determine α_f. First, it is noted that $E[\alpha_f]$ assumes such great values in Fig. 17 compared with those in Fig. 15. It is said that Eq. (53) has been proposed for the case where $T_0=0.3$ sec. Hence to compare Fig. 15 and Fig. 17, the acceleration in Fig. 15 should be multiplied by $(0.3/0.5)^{-1.316}=1.959\cong 2.0$. After this account, however,

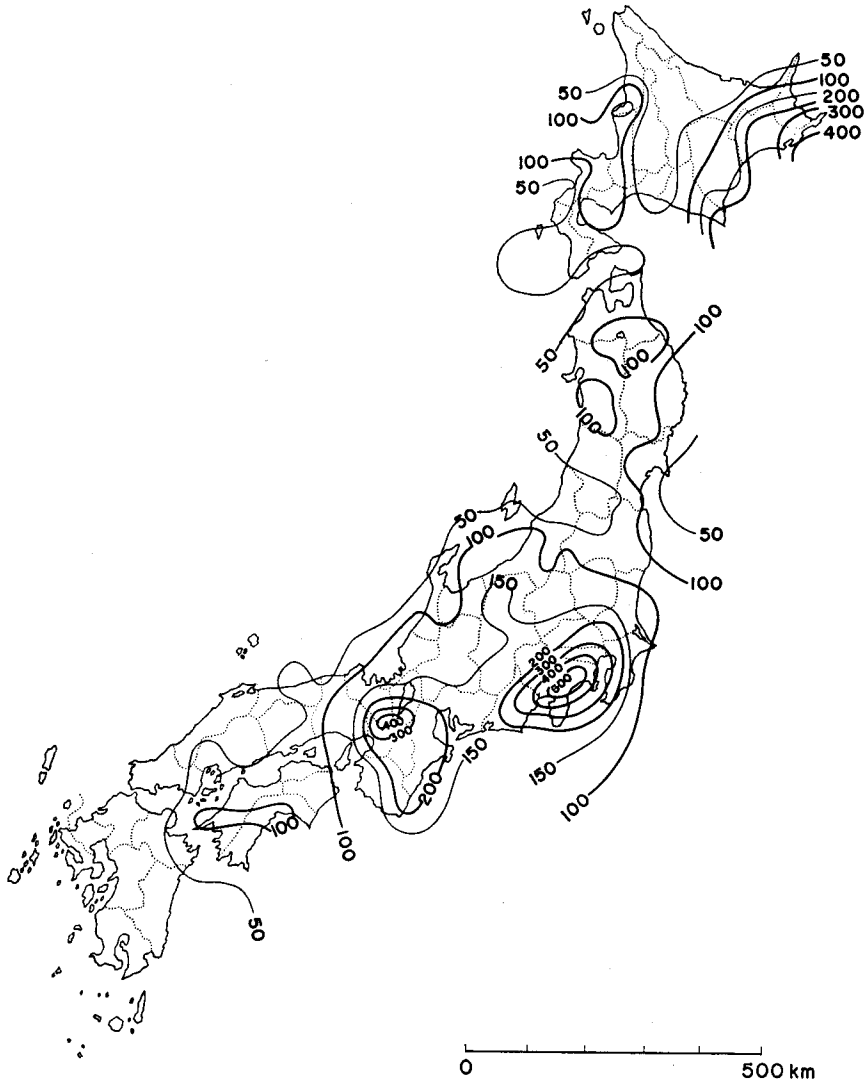

Fig. 18. Seismic Map for the Expected Value of the Maximum Earthquake Acceleration in 75 Years Prepared by H. Kawasumi.

Fig. 17 still shows far greater values than Fig. 15, and they seem to be unrealistically large. This was the reason for proposing Eqs. (56)∼(56″), and the authors would like to suggest that the numerical results shown in the previous section rather than those in this section be refered to for practical use. In this section, however, Fig. 17 is compared with Kawasumi's map shown in Fig. 18, since the latter is also based on Eq. (53).

The greatest theoretical difference between Figs. 17 and 18 is that the former

takes account not only of how many earthquakes have occurred but also when they occurred, while the latter does not consider the possible time-dependence of the record of earthquakes as pointed out in the foregoing chapters. Fig. 17 on the whole gives larger values than Fig. 18 as the result from the record of past earthquakes whose number generally decreases as we date former ages. This tendency is stronger for Tokyo than for Kyoto as we see in Fig. 1. And in addition, Table A–1 tells us that n_{VII} for Tokyo is much greater than that for Kyoto. Hence it would be a natural result that we have a greater value of $\mathrm{E}[\alpha_f]$ for Tokyo than for Kyoto in Fig. 17, while in Fig. 18 they are almost equal. In Fig. 18, Kyoto is one of the most active seismic zones, mainly due to the large number of past earthquakes registered although not very strong. But in Fig. 17, the most active seismic zones in this district are in the area where Gifu, Aichi, Fukui, Shiga and Mie Prefectures meet and in the southern part of Kii Peninsula both of which have been struck by very strong earthquakes before. These results would imply the appropriateness of the method of analysis in the present study.

Finally comparing Figs. 15 and 18, we see that in Fig. 15 the earthquake danger in less active seismic zones is not so small as indicated in Fig. 18. This is observed in the western part of Chugoku District, along the east coast of Kyushu or in the central part of Tohoku District.

5. Conclusions

From the results of the analyses in this study, following conclusions may be derived.

1) With the aid of the statistical model of earthquakes proposed in **2.**, one can make a probabilistic analysis of the maximum ground motion in earthquakes with due consideration of the possible time-dependence of the accuracy of the record of past earthquakes and with that of the randomness of the ground motion.

2) On the basis of this statistical model of earthquakes, methods have been discussed for deriving the probability distribution of the maximum ground motion in a single earthquake and that for a certain future period.

3) It has been proved by a theoretical analysis and the result of numerical simulations that the distribution functions defined by Eqs. (31)$\sim$(36) are good approximations to the probability distributions of the maximum ground motion in a single earthquake.

4) The parameter β (or β_I) discussed in **3.**(2) serves as a direct measure of the earthquake intensity in the structural response analysis in which the structure is to be subjected to an ensemble of earthquakes with a certain assigned r.m.s. intensity.

5) The shape of the probability distribution function of the maximum ground motion in a single earthquake and its expected value are not greatly affected by τ/T_0 in the range $\tau/T_0=10\sim100$ which is of our interest.

6) It can be stated from the numerical results that when a precise probabilistic judgment of the future maximum ground motion in earthquakes is required reference should be made not only to its expected value but also to its distribution function which has a shape particular to the locality under discussion.

7) A rough prediction of the maximum earthquake ground motion in a future period can be made by means of the seismic map showing its expected value. For this purpose the authors recommend to use Figs. 15 and 16 which are based on the method of analysis discussed in this study.

8) The method of analysis of the present study can be elaborated when we have attained more data on earthquakes. For example, accumulation of strong motion seismograph records in the future will give some quantitative idea about the shape of their subsiding tails and enable us to take the effect of nonstationarity into account. By such processes the numerical results given in this paper will be even more accurate.

Acknowledgment

The authors would like to extend their gratitude to Professor Kenzo Toki for his kind advice about the technique of the numerical simulation of earthquakes. It is also acknowledged that the simulation of random earthquakes and most part of other numerical computations were made on the digital computer KDC-II of the Kyoto University Computation Center.

Appendix. Some Basic Data of Earthquakes Used in Numerical Application

Fig. A-1 shows the location and magnitude of earthquakes used in the numerical application in **4**. In Table A-1 are indicated some basic numbers of earthquakes for various classifications. It being impossible to show these data for every locality of Japan because of the limitation to space, only those for localities dealt with for example in Fig. 14 and Table 1 are shown.

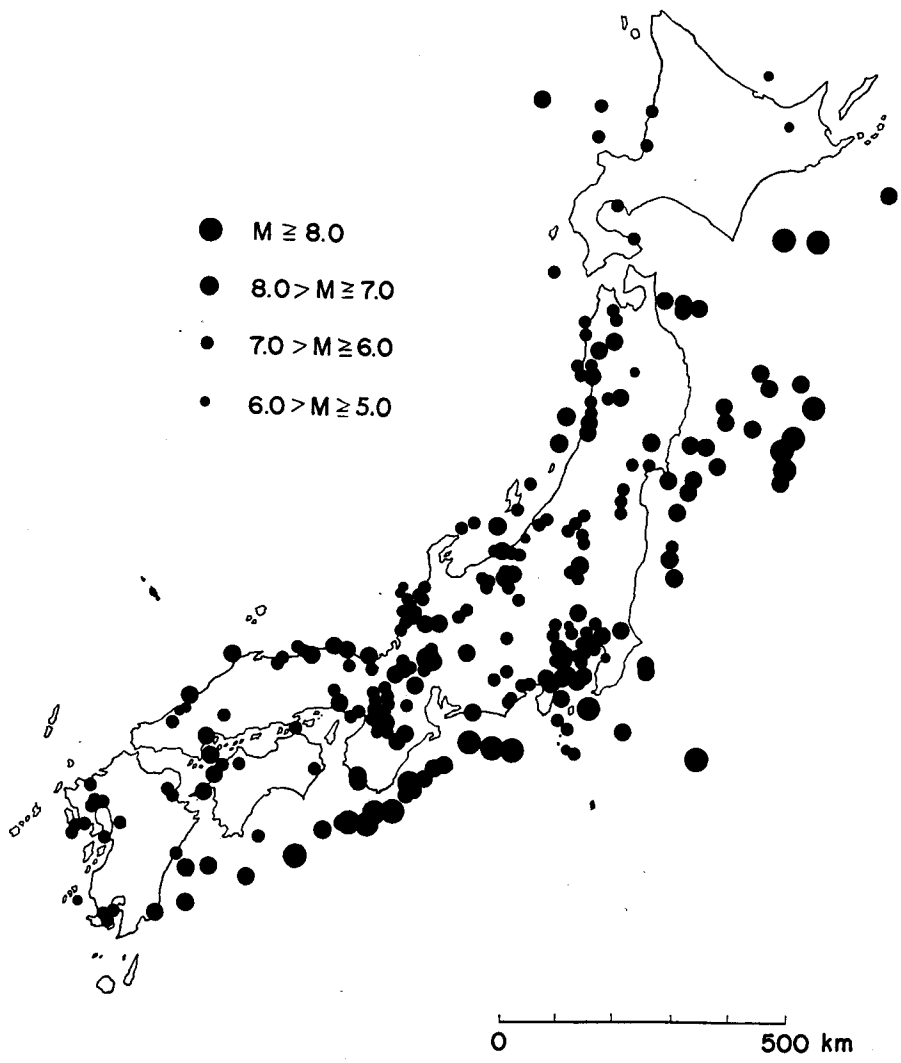

Fig. A-1. Location and Magnitude of Earthquakes.

Table A-1. Examples of Data of Past Earthquakes.

locality	N	n_{V}	n_{VI}	n_{VII}	N_r	S_r (year)
Kushiro	3	1	0	2	3	150
Sapporo	1	1	0	0	1	150
Akita	14	7	6	1	8	200
Sendai	11	9	1	1	7	200
Tokyo	31	14	10	7	15	200
Toyama	14	10	4	0	4	200
Nagoya	19	9	6	4	8	200
Kyoto	39	20	18	1	13	200
Hiroshima	9	5	3	1	4	200
Kochi	9	6	2	1	4	200
Fukuoka	2	2	0	0	1	200
Miyazaki	6	4	1	1	4	200

References

1) Kawasumi, H.; "Measures of Earthquake Danger and Expectancy of Maximum Intensity Throughout Japan as Infered from the Seismic Activity", Bull. Earthq. Res. Inst., Univ. of Tokyo, Vol. 29, pp. 469–482 (1951).
2) Muramatsu, I.; "Distribution of the Maximum Earthquake Velocity in 50 Years throughout Japan", Proc. Conf. Disaster Prevention Science, Tokyo, pp. 201–204 (1965), (Japanese).
3) Ravara, A.; "Spectral Analysis of Seismic Actions", Proc. III WCEE, Vol. 1, pp. III 195–III 204 (1965).
4) Kobori, T. and Minai, R.; "Earthquake Response of Elasto-Plastic Multi-Story Building Structure", Disaster Prevention Res. Inst., Kyoto Univ., Annuals, No. 7, pp. 141–163 (1964), (Japanese).
5) Rice, S. O.; "Mathematical Analysis of Random Noise", Selected Papers on Noise and Stochastic Processes edited by N. Wax, Dover, pp. 133–294 (1954).
6) Coleman, J. J.; "Reliability of Aircraft Structures in Resisting Chance Failure", Operations Research, Vol. 7, pp. 639–645 (1959).
7) Rice, J. R. and Beer, F. P.; "First-Occurrence Time of High-Level Crossings in a Continuous Random Process", Jour. Acoust. Soc. Amer., Vol. 39, pp. 323–335 (1966).
8) Shinozuka, M.; "Probability of Structural Failure under Random Loading", Proc. ASCE, Vol. 90, EM5, pp. 147–170 (1964).
9) Goto, H., Toki, K. and Akiyoshi, T.; "Generation of Artificial Earthquakes on Digital Computer for Aseismic Design of Structures", Proc. Japan Earthq. Engng. Symp. 1966, Tokyo, pp. 25–30, (Japanese).
10) Kanai, K.; "Improved Empirical Formula for the Characteristics of Strong Earthquake Motions", Proc. Japan Earthq. Engng. Symp. 1966, Tokyo, pp. 1–4, (Japanese).
11) Japan Society of Civil Engineers, ed.; "Vibration Handbook for Civil Engineers", JSCE, pp. 147–148 (1966), (Japanese).